Locomotion Control of a Biomimetic Robotic Fish based on Closed Loop Sensory Feedback CPG Model

Deniz Korkmaz[1], Gonca Ozmen Koca[2,*], Guoyuan Li[3], Cafer Bal[2], Mustafa Ay[2] and Zuhtu Hakan Akpolat[4]

[1]Department of Electrical and Electronics Engineering, Faculty of Technology, Firat University, 23119, Elazig, Turkey

[2]Department of Mechatronics Engineering, Faculty of Technology, Firat University, 23119, Elazig, Turkey

[3]Department of Ocean Operations and Civil Engineering, Norwegian University of Science and Technology, Aalesund, Norway

[4]Department of Electrical and Electronics Engineering, Faculty of Engineering, Fatih Sultan Mehmet Vakif University, 34015, Istanbul, Turkey

Corresponding author: *gonca.ozmen@gmail.com

Abstract

This paper presents mechatronic design and hierarchical locomotion control of a biomimetic robotic fish for three-dimensional swimming modes. Inspired by biological features of Lamprey, a closed loop sensory feedback Central Pattern Generator (CPG) model is adapted to hierarchical control mechanism in order to provide robust and effective biomimetic control structure. A sensory feedback mechanism plays an important role to react external stimuli from environment. In addition, a closed loop fuzzy logic control structure is developed as a brain model to decide adaptive swimming modes according to sensory information. In order to provide three-dimensional motion abilities, the Center of Gravity (CoG) control mechanism is designed and controlled by a back-forth proportional control structure. Experimental results are obtained to prove the CPG-based closed loop sensory feedback control structure with the developed robotic fish prototype.

Keywords: robotic fish; central pattern generator; sensory feedback; closed loop control; fuzzy logic

1. Introduction

Vertebrate animals exhibit various motor patterns such as walking, running, crawling, swimming and flying. They achieve these efficient patterns by coordinated muscles in the skeletal system. The locomotor behaviors performed by the body can be created by neurons in the spinal

cord without any stimulus from higher control center or sensory receptors. These special neurons are described as Central Pattern Generators (CPGs) in the literature. CPGs are the biological neurons that generate oscillatory rhythmic outputs to provide locomotion patterns (Lachat et al. 2006; Ijspeert et al. 2005; Wu et al. 2012; Li et al. 2014a; Bing et al. 2017; Wang and Hu et al. 2013).

Adding synchronous and non-linear motion properties observed in the living muscles to each joint of a robot with more than one joint has always been an important problem in the field of robotics (Wang et al. 2013; Wang et al. 2017; Yu et al. 2016). In order to provide effective mobility, a CPG model can easily generate behaviors based on different physical properties such as position, force, torque, muscle length, speed and frequency; and protect these outputs against external disturbances. Also, artificial CPG-based controllers exhibit the similar intrinsic coordinated, steady and robust properties to those natural CPGs in vertebrates. These excellent features show that CPG-based control methods have begun to be used alone and/or together with other control methods for uncertain locomotor behavior. In addition, a neuronal CPG circuit has become more and more popular topic for a new generation of control due to its elegant, efficient, stable, adaptable and hierarchical system solutions for various robotics and engineering systems (Wang et al. 2005; Wu et al. 2009; Ding et al. 2013; Wu et al. 2014).

When swimming robots are investigated in the literature, it can be seen that many different CPG-based locomotion controllers are used. These controllers can be divided into two main categories: open loop and closed loop CPG models (Korkmaz et al. 2018). Open loop CPG control methods generally concentrate the generation of multiple swimming behaviors. Zhang et al. performed the forward, backward and turning swimming motions of a six-joint robotic fish model with nonlinear Zhang oscillators in a simulated environment (Zhang et al. 2006). Wang et al. demonstrated the ring-coupled linearized amplitude controlled phase oscillators to generate forward and backward motions of a three-joint robotic fish (Wang and Xie 2014). Ijspeert designed Lamprey oscillator model to generate salamander robot motions (Ijspeert 2008). Crespi examined the forward and turning motions of a single articulated ostraciiform robotic fish with amplitude controlled phase oscillators (Crespi et al 2008; Lachat et al. 2006). Hu et al. developed a single-joint robotic fish with Hopf oscillators and they examined the speed performance due to frequency variations (Hu et al. 2015). Also, Niu et al. designed Anguilliform robotic fish and performed open loop swimming performance with Andronov-Hopf oscillators connected in a three-dimensional ring model (Niu et al. 2014). Yu et al. determined the CPG parameters with particle swarm optimization to obtain the optimum speeds in different type swimming modes (Yu et al. 2016). In contrast, closed loop CPG-based controllers generally adapts the feedback mechanism in the CPG network to generate necessary locomotor behaviors according to the environmental changes, which mimics the real mechanism of animal CPG activities. Examples are not quite much on robotic fish. Wang et al. performed trajectory tracking control of an

ostraciiform type robotic fish by changing amplitude, offset and frequency of amplitude controlled phase oscillators. In order to increase the success of the tracking performance, yaw, pitch and roll angles were also controlled (Wang et al. 2013; Wang and Xie 2014). Zhang et al. developed a robotic fish and examined both BCF and MPF motions with Hopf oscillators. They also performed three-dimensional motion control of the robot to avoid obstacles (Zhang et al. 2016). Also, yaw angle control is performed with amplitude controlled phase oscillators combined with the traditional PID controller (Wang and Xie 2014).

A sensory feedback and closed loop controller is an important model for determining the locomotor patterns according to environmental factors and it realizes swimming pattern transitions, synchronization and stability. In addition, these types of CPGs can provide modulated motor outputs based on received stimulus from sensory neurons and they exhibit similar biological CPG characteristics. Unfortunately, due to complexity of the biological based CPG models and difficulties of real-time microprocessor implementations, the closed loop sensory feedback CPG controllers have been less examined in fish-like swimming locomotion of underwater robots. Especially, adaptive and hierarchical design methods for sensory feedback are still incomplete (Li et al. 2014b; Wang and Xie 2014; Yu et al. 2014).

The main contribution of this paper is to develop a hierarchical control mechanism based on a closed loop sensory feedback CPG model to perform real-time three-dimensional multimodal swimming motions of a robotic fish in the experimental pool. A biomimetic, carangiform type, autonomous robotic fish with two-link propulsion tail mechanism (i-RoF) is designed and developed. As the basis of the hierarchical control mechanism, the CPG model based on Lamprey spinal cord from (Li 2013) is utilized to provide robust and stable biomimetic control structure. A sensory neuron mechanism is adapted to the CPG model to perceive external stimuli from environment. In addition, a closed loop fuzzy logic controller is designed as a brain model to determine adaptive swimming patterns according to sensory information. In order to perform up/down motions, a Center of Gravity (CoG) control mechanism is developed and it is controlled with a simple and highly applicable controller. Experimental results are provided to validate the CPG-based closed loop sensory feedback control method with the developed i-RoF prototype.

This paper provides five main sections. The literature review about the CPG-based locomotion control of the robotic fish is given in Section 1. The developed robotic fish prototype is briefly presented in Section 2. The framework of the hierarchical control structure and the detailed CPG model with sensory feedback mechanism are presented in Section 3. The designed closed loop control structure is described in Section 4 and Section 5 shows the experimental results. Finally, conclusions and some suggestions for future works are given in Section 6.

2. Mechatronic Design of the Robotic Fish Prototype

In this section, a two-link carangiform biomimetic robotic fish prototype (i-RoF) which is developed by the authors (Ozmen Koca et al.2017; Ay et al. 2018; Ozmen Koca et al. 2018) is given with mechanical, electronic and sensor structures. The developed robotic fish exhibits following characteristics: 1) three-dimensional swimming; 2) high speed performance; 3) biomimetic control based swimming ability; 4) capability of performing the determined tasks.

2.1. Mechanical Design

As shown in Figure 1, i-RoF is designed with modular parts and it consists of a well-streamlined anterior rigid main body, two-link propulsive tail mechanism, front sight unit and a flexible caudal fin. Dimensional and characteristic specifications of all parts are determined according to a carangiform carp fish. CoG control mechanism is located to main body to generate up/down swimming motions. This mechanism consists of a sliding mass along the horizontal *x* axis and a RC servo motor.

Thrust force of the robotic fish is generated by the designed serial two-link tail mechanism. Each link is driven by powerful RC servo motor and flexible tail mechanism is fixed to the peduncle. In order to avoid the dynamic obstacles, the front sight unit is designed with three distance sensors placed horizontally parallel to each other in the *x* axis. In the prototype design, static and dynamic sealing are provided for long-term waterproofness.

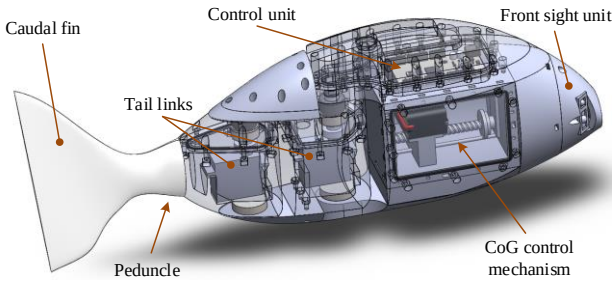

(a)

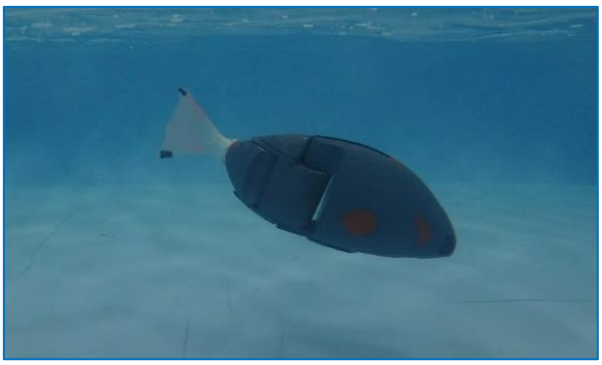

(b)

Figure 1. Mechanical and hardware configurations of the robotic fish: (a) Concept design; (b) Robotic fish prototype (i-RoF)

Each servo motor of the tail link is located to the designed motor bed and an aluminum 25T upper shaft is mounted to the motor gear to transmit turning motion. A sealing ring and a roller are also mounted to each shaft to keep out the water while shaft is rotating. At the same time, O-ring channels are designed in all parts to provide waterproof structure and all surfaces are also mounted by coating fluid sealing. Finally, these parts are covered with epoxy resin to prevent possible leakages.

2.2. Electronics and Sensors

Electronic system of the robot includes control unit, power supply, communication, environmental sensors and servo motors as shown in Figure 2. A 7.4 V 1350 mAh Lithium-Polymer (Li-Po) rechargeable battery, which is preferred for robotic applications due to its smaller size with high capacity, is used for power supply of the robotic fish and a power distribution circuit is designed to convert necessary voltage values of all elements. Bluetooth HC-06 module is adopted for wireless communication between the robotic fish and user computer via RX/TX serial protocol. Communication distance is approximately 10 m and this unit is active when the robotic fish is swimming near the water surface.

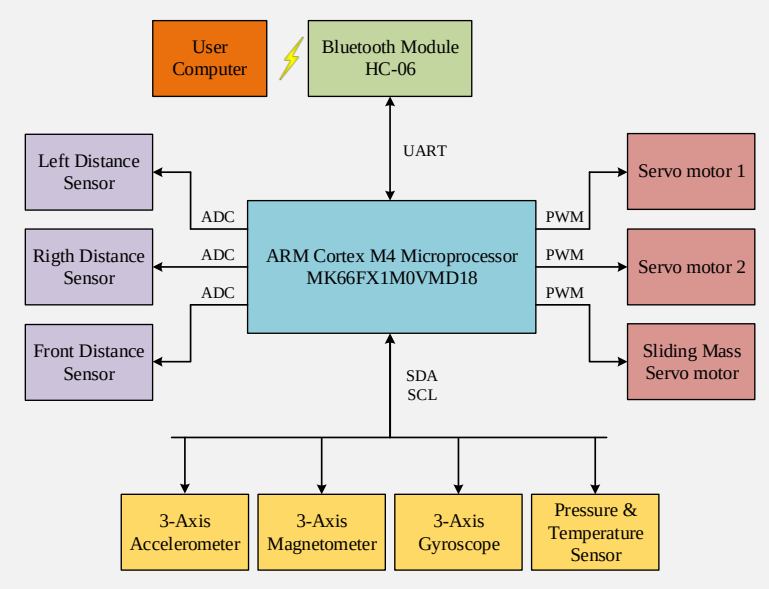

Figure 2. Block diagram of the electrical system

10-DoF IMU module is used to measure Euler yaw, pitch and roll angles and determines the linear and angular speeds according to the Earth-fixed frame. IMU module has a FX0S8700CQ 6-axis accelerometer and compass sensor, a FXAS21002C 3-axis gyroscope and a MPL3115A2 pressure and temperature sensors. Communication between IMU and microcontroller is ensured with I^2C. There is a 32 bit 180 MHz ARM Cortex M4 MK66FX1M0VMD18 microcontroller to perform rhythmic oscillatory swimming motions. The front sight unit consists of three sight

distances as left, front and right. Each sensor is infrared Sharp GP2Y0A21YK0F and distance range is 6 - 80 cm. Obstacle detection angle of the sensors are nearly 40°. Technical specifications of the developed robotic fish prototype are listed in Table 1.

Table 1. Technical specifications of i-RoF

Items	**Characteristics**
Dimensions (L x W x H)	~ 500 mm x 76 mm x 215 mm
Total Mass	~ 3.1 kg
Tail Driving System	Servo motor (29 kg.cm, 7.4 V)
CoG Driving System	Continuous servo motor (12 kg.cm, 7.4 V)
Sensors	10-DoF IMU, infrared distance sensors,
Power Supply	7.4 V, 1350 mAh rechargeable Li-Po battery
Operation Time	~ 30 min
Swimming Ability	Autonomous, user-controlled
Motion Ability	Three-dimensional

The robotic fish is approximately 500 mm long, 76 mm wide and 215 mm high. The prototype mass is also approximately 3.1 kg.

3. Framework of the Hierarchical Locomotion Control

In this paper, a hierarchical closed loop control structure based on a sensory feedback CPG model is proposed to perform real-time three-dimensional swimming motions of a carangiform robotic fish prototype. The proposed CPG model is designed based on Lamprey spinal cord to provide rhythmic, coordinated and stable BCF swimming motions. A sensory neuron mechanism is adapted to CPG to perceive external stimuli with onboard sensors. The closed loop fuzzy logic controller is also developed to determine necessary swimming patterns according to sensory information. With the designed CPG model, brain stem and spinal cord model of the robotic fish is established. Also, upper brain center model of the robotic fish is designed with the fuzzy controller and this closed loop hierarchical control structure behaves as the Central Nervous System (CNS) model of the robot prototype in real-time as shown in Figure 3.

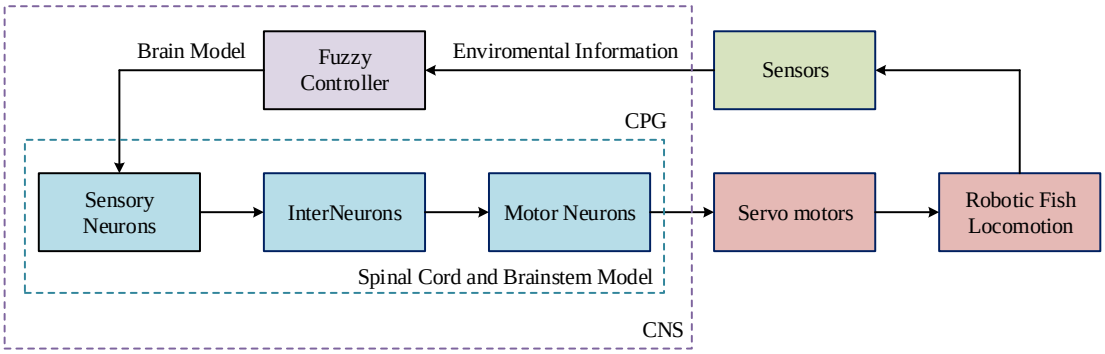

Figure 3. The designed CNS model of the robotic fish based on closed loop sensory feedback CPG model

Multimodal swimming motions are generated with the proposed closed loop controller according to environmental situations and/or given tasks.

3.1. CPG-Based Biomimetic Spinal Cord Model

The neural CPG network consists of a Motor Control Unit (MCU) and a series of chain oscillators, which generate rhythmic oscillatory outputs. MCU acts like a brainstem of the CPG and it sends motor commands to oscillators to modulate the phase differences of the outputs. As shown in Figure 4, a neural Lamprey oscillator is divided into two basic parts which are left and right symmetrical sections to each other. There are three interneurons namely Crossed InterNeurons (CIN), the Lateral InterNeurons (LIN) and the Excitatory InterNeurons (EIN) and a Motor Neuron (MN) in both sections. Rhythmic oscillatory activities are provided with interaction of these neurons. At the same time, each oscillator is interconnected by external coupling synapses. An oscillator sends inhibitory synapses to other oscillators by EINs. Each LIN receives incoming synapses from other oscillators. It is noted that presynaptic neuron in an oscillator and postsynaptic neuron in another oscillator are on the same side as the left and right sections.

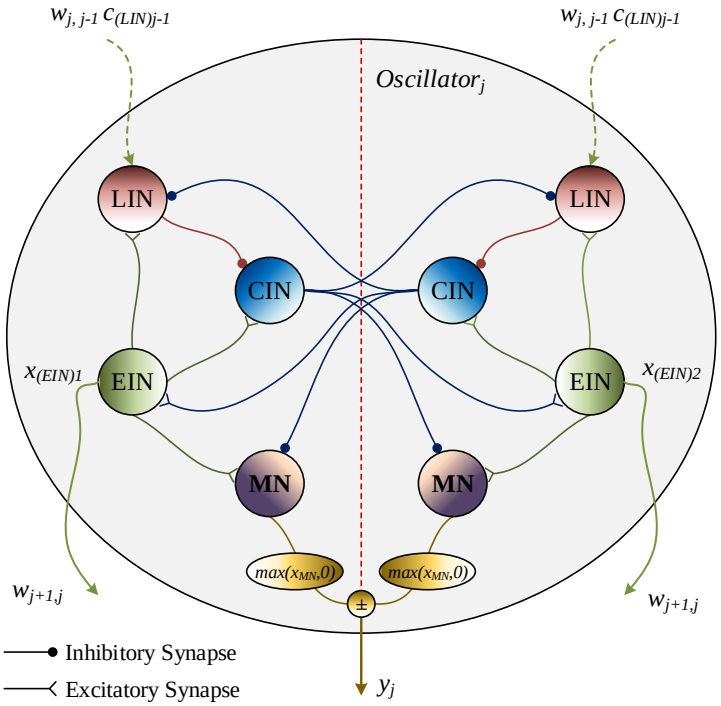

Figure 4. The designed neural single Lamprey oscillator. Each oscillator is connected with synaptic weights from EIN to LIN

In the oscillator model, the interneurons occur from a series of Leaky Integrate and Fire (LIF) cells. The LIF cell model describes a little change in the membrane potential of a cell in time-varying and it is also one of the simplest spiking neuron model. In the designed oscillator, each CIN can defined as;

$$\tau \dot{x}_{(CIN)i} = -x_{(CIN)i} + \sum_{k=1}^{n} w_{i,k} s_{(CIN)i,k} \qquad \{i = 1,2; \quad j = 1,2,...,N; \quad k = 1,2,...,n\} \tag{1}$$

The LIN and EIN interneurons are expressed as Equation (2) and (3), respectively;

$$\tau \dot{x}_{(LIN)i} = -x_{(LIN)i} + \sum_{k=1}^{n} w_{i,k} s_{(LIN)i,k} + \sum_{j=1}^{N} w_{j,j-1} c_{(LIN)j-1} \tag{2}$$

$$x_{(EIN)i} = \frac{A}{1 + e^{x_{(CIN)}}} - \frac{A}{2} \tag{3}$$

The MN can be given by;

$$\tau \dot{x}_{(MN)i} = -x_{(MN)i} + \beta A + \sum_{k=1}^{n} w_{i,k} s_{(MN)i,k} \tag{4}$$

and thus, the oscillator output is obtained as below;

$$y_j = \max\left(x_{(MN)1}, 0\right) - \max\left(x_{(MN)2}, 0\right) \tag{5}$$

In these equations, i is left and right parts belonging to the oscillators, j is the number of oscillator and k is the number of neurons in each oscillator. The upper line of the lower symbol defines the opposite side in the same oscillator. x_i is the membrane potential of the neurons and y_j is the oscillator output. τ, β and A determine the period, offset and amplitude of the oscillator output, respectively. w_{ik} and w_{ij} are the synaptic weights of the neurons and synaptic weights of the oscillators, respectively. s_i is the presynaptic neuron potentials in the same oscillator and s_i with w_{ik} are the amount of the neurotransmitter transferred to the postsynaptic neuron. c_j is the presynaptic neuron potential in the other oscillator and c_j with w_{ij} also give the amount of the neurotransmitter transferred to the postsynaptic neuron in the other oscillator.

It can be seen from Equation (3) that EIN type neuron is different from the equation of LIF neuron model. There is a sigmoid function with a threshold value A. EINs in an oscillator emit excitatory synapses to other neurons on the same side and the sigmoid function provides constantly changes of the membrane potential of neurons. As a result, rhythmic oscillatory outputs in the steady state are occur.

Based on the biological structure of carangiform type fish, lateral motion defined as body traveling wave smoothly increases from nose to tail. Thus, the phase relation in the designed tail mechanism of the robot is an important key point on the fish locomotion and there is always a phase lag between the links of tail to provide the body traveling wave during swimming as illustrated in Figure 5. In the CPG model, phase differences of the outputs are determined with MCU. The neural MCU acts as a brainstem in the spinal cord and it emits inhibitory synapses to the oscillators according to the determined connection topology. MCU is designed with the use of two additional synapses ($w_{R,L}$, $w_{L,R}$) in an oscillator model. $w_{R,L}$ is the inhibitory synapse outgoing from the left EIN to the right LIN and $w_{L,R}$ is the excitatory synapse outgoing from the right EIN to the left LIN. The phase difference between the oscillators are adjusted with these two additional synapses. In order to precisely adjust the phase differences, $w_{R,L}$ and $w_{L,R}$ should be in the range (0,1] and [-1,0), respectively and these are determined by the following expression:

$$\begin{bmatrix} w_{L,R} & w_{R,L} \end{bmatrix} = \begin{bmatrix} \dfrac{\alpha}{\alpha+\gamma} & \dfrac{-\gamma}{\alpha+\gamma} \end{bmatrix} \tag{6}$$

In this expression, α and γ are the phase relation coefficients and their values change in the range of (0,1].

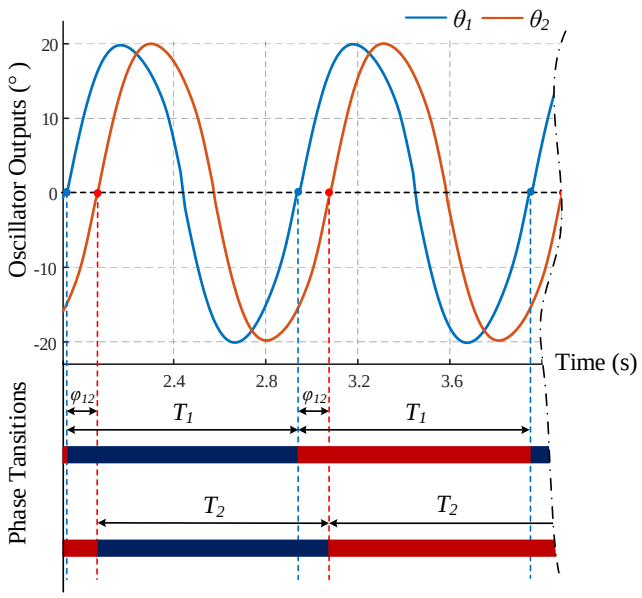

Figure 5. Phase transitions between two oscillators adjusted by MCU

In order to obtain rhythmic and smooth sinusoidal oscillator outputs, all internal weights have a value of 1 and the internal weight from EIN to MN has also value of 0.1. At the same time, the initial value of a neuron plays an important role in the generation of rhythmic oscillations. A self-sustaining oscillator output is obtained when the initial condition is determined by a very small difference between the left and right CINs that emit inhibitory synapses to other neurons except EIN.

An illustrative scenario of how CPG outputs react to the parameter change is shown in Figure 6. Five locomotion patterns are performed for forward and turning swimming modes during 50 s. $t \in [0 - 10]$ s, $t \in (10 - 20]$ s and $t \in (20 - 30]$ s intervals show the forward swimming motions. Also, $t \in (30 - 40]$ s and $t \in (40 - 50]$ s intervals describe the left and right turning swimming motions, respectively. During simulation, two different phase difference are used. γ is fixed to 0.2 and thus α is the only parameter changed for phase lag. Oscillation amplitudes are determined as (10°, 20°, 30°). Flapping frequencies depending on τ parameters are chosen as 2 Hz, 1 Hz and 0.75 Hz, respectively.

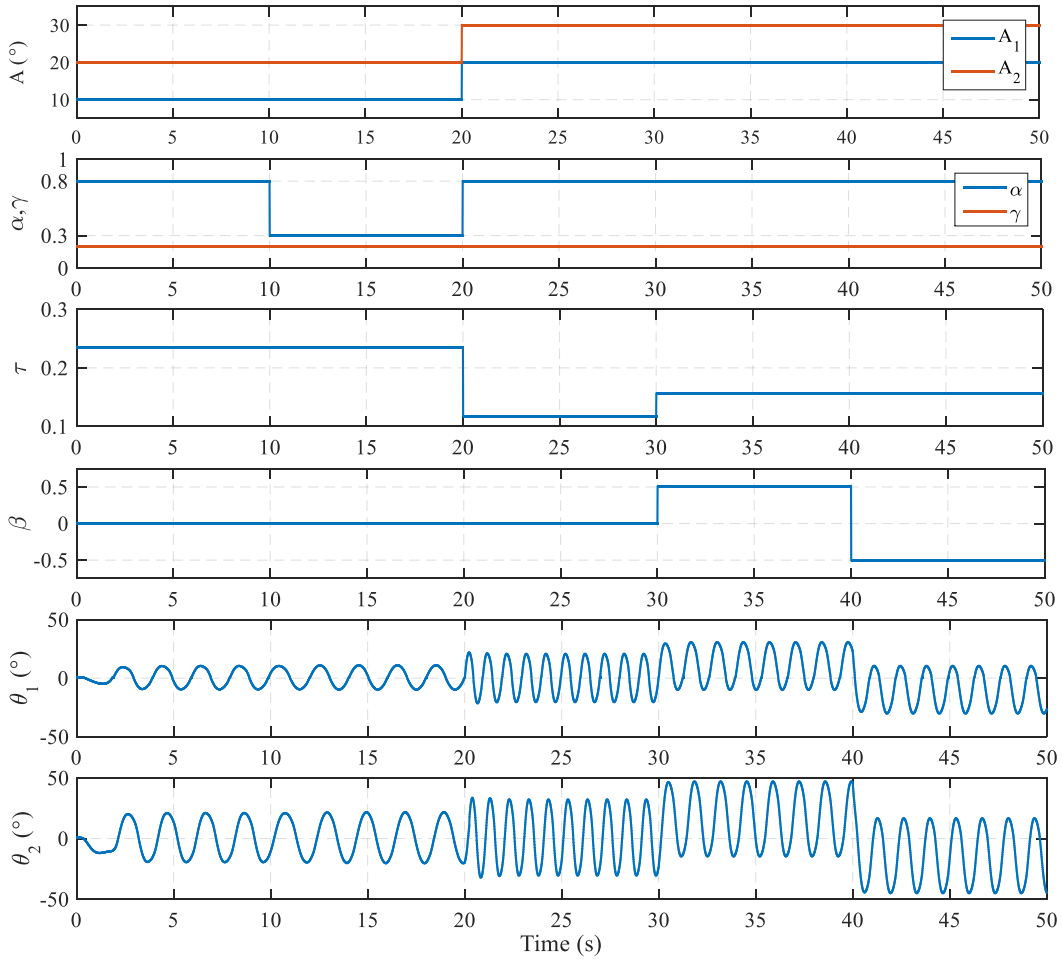

Figure 6. CPG Outputs against parameter variations

It is clear that when the parameters suddenly changed, CPG network can still converge smoothly and rapidly to the new swimming motion without failure. While robotic fish is swimming in water, transitions among different locomotion patterns are necessary according to expected tasks and environmental conditions. In these events, smooth, fast and robust transactions are the key point. Otherwise, jerky motions occur, which can break the mechanical parts of servo and fish-like swimming cannot be obtained. Thus, instantaneous signal transitions should be avoided.

In this part of study, the smoothness and efficiency of CPG outputs are analyzed during transitions between different locomotion patterns. Same parameter changes are performed and compared between the outputs from oscillator and from sinusoidal functions. For different time intervals, different parameters are chosen corresponding to different locomotion patterns and two scenarios are performed for link angles θ_1 and θ_2. Table 2 gives time intervals and simulated scenarios for amplitude, frequency and offset changes according to these intervals. The scenarios for the first and second links are shown in Figure 7.

Table 2. Parameter values for generated sinusoidal functions (θ_1^s, θ_2^s) and CPG oscillation outputs (θ_1, θ_2)

First Scenario				
θ_1^s Time (s)	θ_1 Time (s)	Amplitude (°)	Frequency (Hz)	Offset (°)
[0 - 10]	[0 - 10]	20	0.5	0
(10 - 20]	(10 - 20]	20	0.25	0
(20 - 30]	(20 - 30]	10	0.25	0
(30 - 40]	(30 - 40]	20	0.5	0
(40 - 50]	(40 - 50]	20	0.5	-10
Second Scenario				
θ_2^s Time (s)	θ_2 Time (s)	Amplitude (°)	Frequency (Hz)	Offset (°)
[0 - 10]	[0 - 9.10]	30	0.5	0
(10 - 20]	(9.10 - 18.31]	30	0.25	0
(20 - 30]	(18.31 - 30.27]	20	0.25	0
(30 - 40]	(30.27 - 38.68]	30	0.5	0
(40 - 50]	(38.68 - 50]	30	0.5	+15

For the first scenario, both the oscillator output and sinusoidal function are changed at the same time intervals. Amplitude is 20°, flapping frequency is 0.5 Hz and offset is 0° at $t \in$ [0 - 10] s; amplitude and offset remain the same and flapping frequency is 0.25 Hz and offset is 0° at $t \in$ (10 - 20] s; flapping frequency and offset remain the same and amplitude is 10° at $t \in$ (20 - 30] s; offset is the same, amplitude is 20° and flapping frequency is 0.5 Hz at $t \in$ (30 - 40] s; finally, amplitude and flapping frequency are the same and offset is -10° at $t \in$ (40 - 50] s. It can be seen that transitions of oscillator output are smooth but sinusoidal function are quite sharp.

According to the second scenario, parameter changes are performed at peak points in the second link. It can be seen that sinusoidal function is distorted and the transitions of the events are quite sharp and instantaneous but oscillator output is quite smooth.

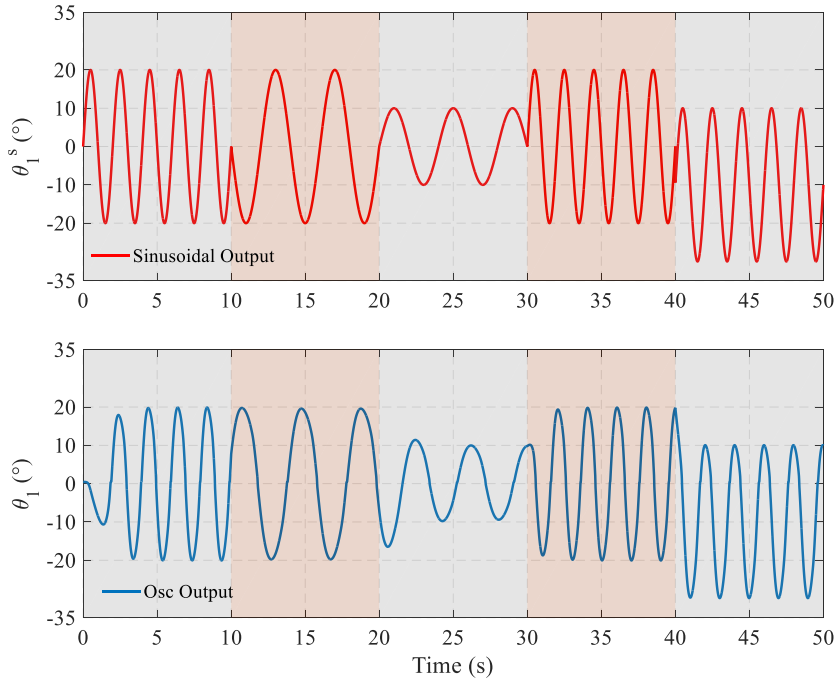

(a)

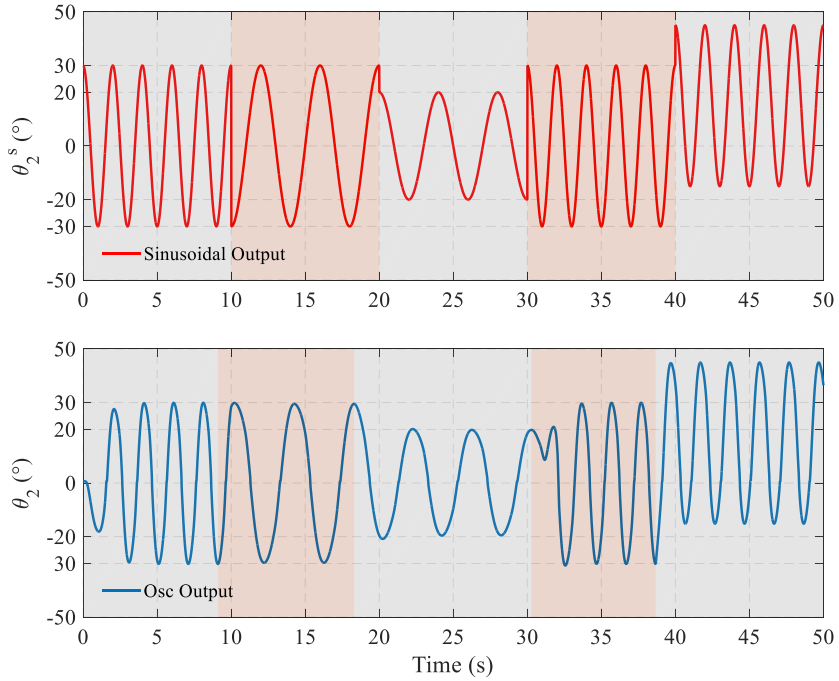

(b)

Figure 7. Transition trajectories with different locomotion patterns as mentioned at Table 2 for (a) first link scenario; (b) second link scenario

Thus arbitrary flapping frequency, oscillation amplitude and offset can be obtained through modulating corresponding parameters and rhythmic, smooth and expected transitions occur depending on these modulations.

3.2. Sensory Feedback Mechanism

The environmental data obtained by the sensors during swimming of the robotic fish are evaluated and the λ parameter which is the stimulus input of the SN is decided by the necessary fuzzy controller according to the robotic fish locomotion determined by the decision mechanism. The interpreted stimulus received by the SNs is transmitted to the CPG model and the response produced by the robot fish and its output is transmitted to the servo motors via MNs. Thus, the swimming motions of the robot are obtained according to the desired control behavior.

In the designed sensory feedback Lamprey CPG oscillator, each SN is defined by the following equation:

$$\begin{cases} \tau_{res}\dot{x}_{(SN)i} = -x_{(SN)i} + p\lambda & \Lambda \le \lambda \\ \tau_{rec}\dot{x}_{(SN)i} = -x_{(SN)i} & \Lambda > \lambda \end{cases} \tag{7}$$

Here, $x_{(SN)i}$ is the membrane potential of SN, τ_{res} is the rise time constant of the response generated to the stimulus, τ_{rec} is the fall time constant of the response generated to the stimulus, p is the correction coefficient of the stimulus, λ is the stimulus amount and Λ is the threshold value. The threshold value determines when external stimuli has become important and the response has to be produced. When the amount of stimulus is greater than or equal to the threshold value, the SN produces an output. Otherwise, the SN output is zero. In the proposed sensory feedback CPG model, each SN emits excitatory synapses to all MNs. In the experimental studies, $\tau_{rec} = 0.4$, $\tau_{res} = 0.1095$, $p = 2$ and $\Lambda = 1$ are determined for parameters of the SN. Also, the parameter values of the SNs in the left and right sections are equal to each other.

4. Closed Loop Control Structure

As shown in Figure 8, the sensory feedback closed loop control system is developed in order to obtain the closed loop control performance of i-RoF. The specific features of the proposed system with sensory feedback CPG model are as follows: 1) the proposed CPG allows the suitable solution for easy integration of sensory feedback mechanism based on neurobiological structure in real-time applications; 2) the developed closed loop control system behaves as an artificial CNS model and performs autonomous swimming against external disturbances; 3) through fuzzy controller, sensory information is analyzed and transferred to the CPG model as sensory input; 4) up/down motions can be easily performed with designed conventional controller.

Obstacle and position data of the robotic fish are received through three distance sensors and one IMU sensor. These data are filtered by the Environmental Data Processing Unit (EDPU) and converted into meaningful values. Mahony [5] for the IMU data and a software filter for the distance sensor data which converts the linear measurement range to the distance values are used.

Decision Mechanism-Motion Combination Unit (DMCU) sends the sensor feedback information from the EDPU to the appropriate control units according to the task definition and also generates the appropriate values of the CPG input parameters (A, τ and α). The turning angle of the robotic fish is determined with parameter λ. The priority of control outputs is decided with the Finite State Machine (FSM). At the same time, the combination of motion is provided with FSM, which is performed multi tasks in the same cycle. It should be noticed that we have only presented yaw, pitch and depth control in this paper because of the limited space. Comprehensive experiments of the autonomous swimming motions with multi tasks using FSM will be presented in a forthcoming paper.

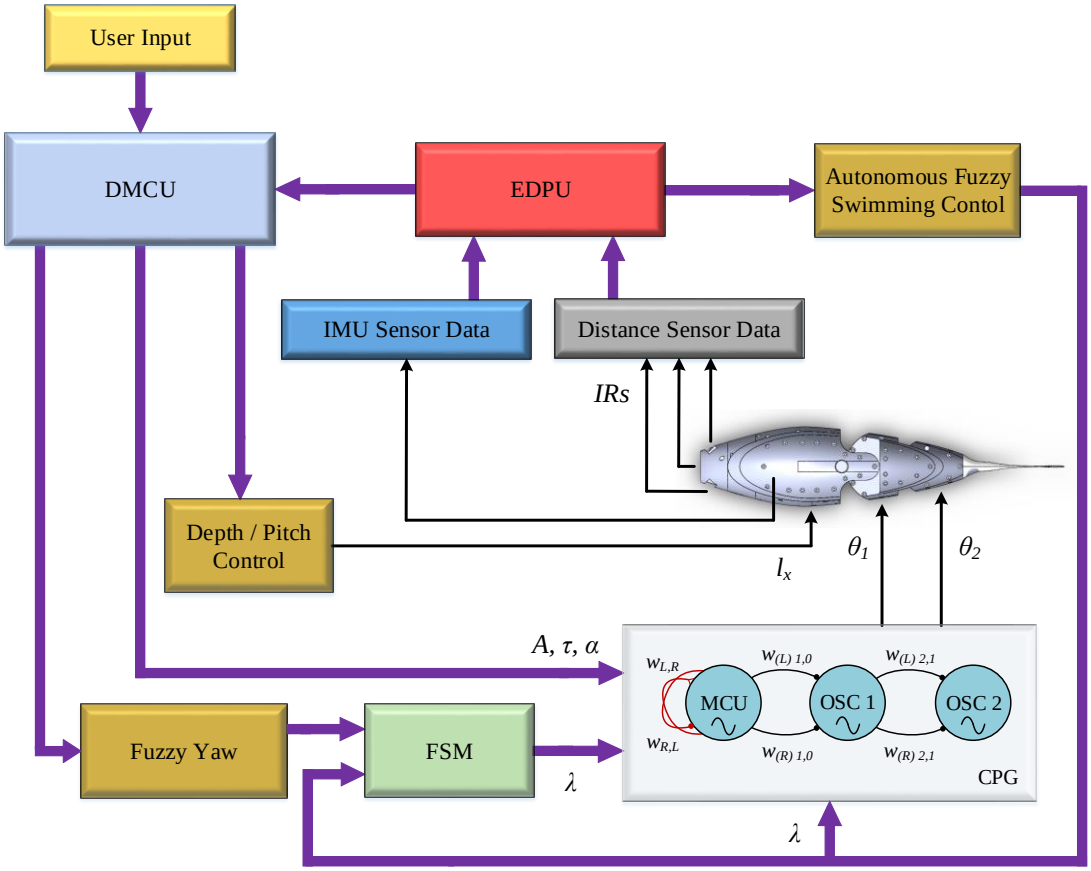

Figure 8. The block diagram of the sensory feedback closed loop control system

The servo motor angles are determined with the output of the CPG model. The position of the moving mass in the CoG control mechanism is changed by Depth Control Unit to provide three-dimensional motion capability. The vertical instantaneous position of the robotic fish at the Earth-fixed frame is determined by the IMU sensor. The back-forth proportional control structure is used for position control of the moving mass.

The CoG of the robotic fish is balanced in the same vertical direction of the lifting center and further below. For this reason, the volumetric distributions of the hardware components are

symmetrical to each other in the horizontal axis and they are also positioned more densely in the vertical axis towards the lower part of the main terminal. This distribution is successfully performed and the control of the roll angle is neglected because it is around 0°.

As noted above, λ parameter, the output of the fuzzy controllers, is the excitatory input value of the feedback neuron, inspired by a real SN that is used to convert the CPG model to a closed loop control scheme with sensory feedback. In order to guide the robotic fish to the desired direction, the closed loop yaw control scheme is designed as shown in Figure 9. λ parameter is determined by evaluating yaw angle values received from the IMU sensor according to the reference values and offset value of the link angles is obtained from output of SN. Thus, the variation of the yaw angle due to β is controlled by the closed loop structure.

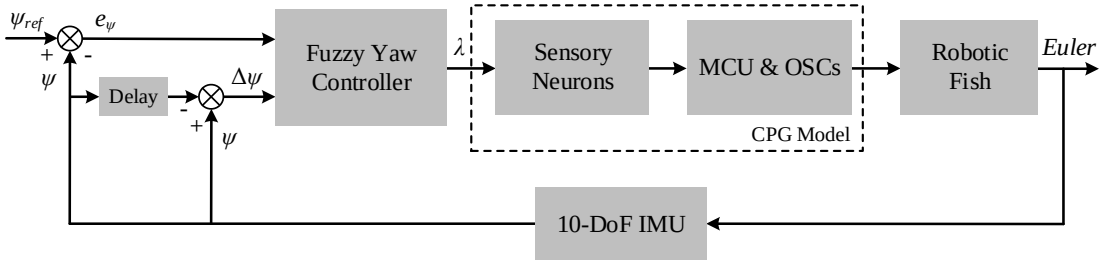

Figure 9. The closed loop yaw control scheme

According to the structure of the system, Mamdani type controller is preferred as fuzzy controller. As the input variables of the fuzzy controller, the error of the yaw angle and the variation of the yaw angle are selected. For a faster response of the control structure, the variation of the yaw angle is preferred instead of the derivation of the error. The input and output membership functions of the fuzzy controller are given in Figure 10.

The value ranges of the membership functions are determined using the characteristics obtained from the open loop performances of the robot. Since the control of the yaw angle changes in the range [-90, 90] for forward motion, the input membership functions are also defined in this range. Parameters of the CPG are determined as $A_1 = 20$, $A_2 = 20$ for amplitude, $\tau = 0.0779$ for the tail flapping frequency of $f = 1.5$ Hz and $\alpha = 0.8$ for the phase difference 45°. According to these values, in order to limit the β parameter to be within the range [-1, 1], the input variable λ parameter of the CPG which provides the change of the yaw angle is selected in the range [-2.5, 2.5].

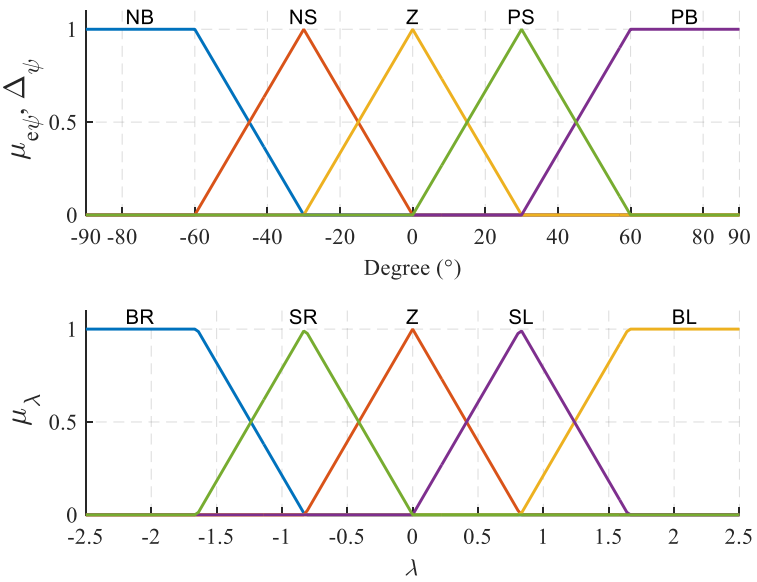

Figure 10. The input and output membership functions of the yaw control. Input membership functions: Negative Big (NB), Negative Small (NS), Zero (Z), Positive Small (PS) and Positive Big (PB) depending on the degrees of yaw angles. Output membership functions: Big Right (BR), Small Right (SR), Zero (Z), Small Left (SL) and Big Left (BL) depending on the robotic fish motion

The rule base of the fuzzy controller for the output variation according to input variables is given in Table 3.

Table 3. The fuzzy rule base

λ		$\Delta\psi$				
		NB	NS	Z	PS	PB
e_ψ	NB	BR	BR	SR	SL	SL
	NS	BR	SR	SR	SL	SL
	Z	SR	SR	Z	SL	SL
	PS	BL	SL	SL	SR	SR
	PB	BL	SL	SL	SR	SR

5. Experiments and Discussion

Three-dimensional motion capabilities of the robot are analyzed with control of the yaw and pitch angles to demonstrate closed loop control performances. The representation of the experimental set is given in Figure 11.

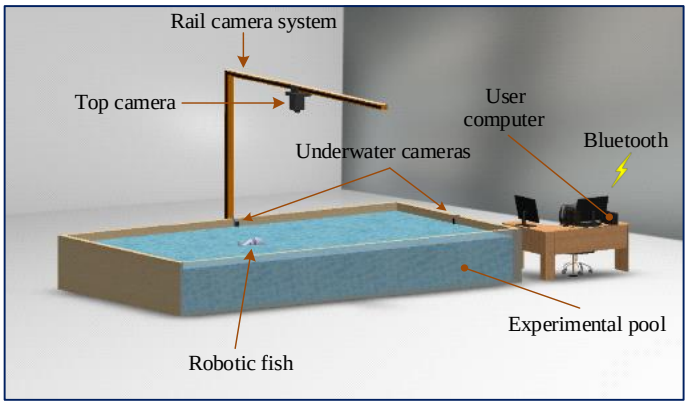

Figure 11. Experimental setup

The yaw control experiments are performed for three different reference angles (15°, 30°, 45°) and snapshots of these experiments are presented in Figure 12.

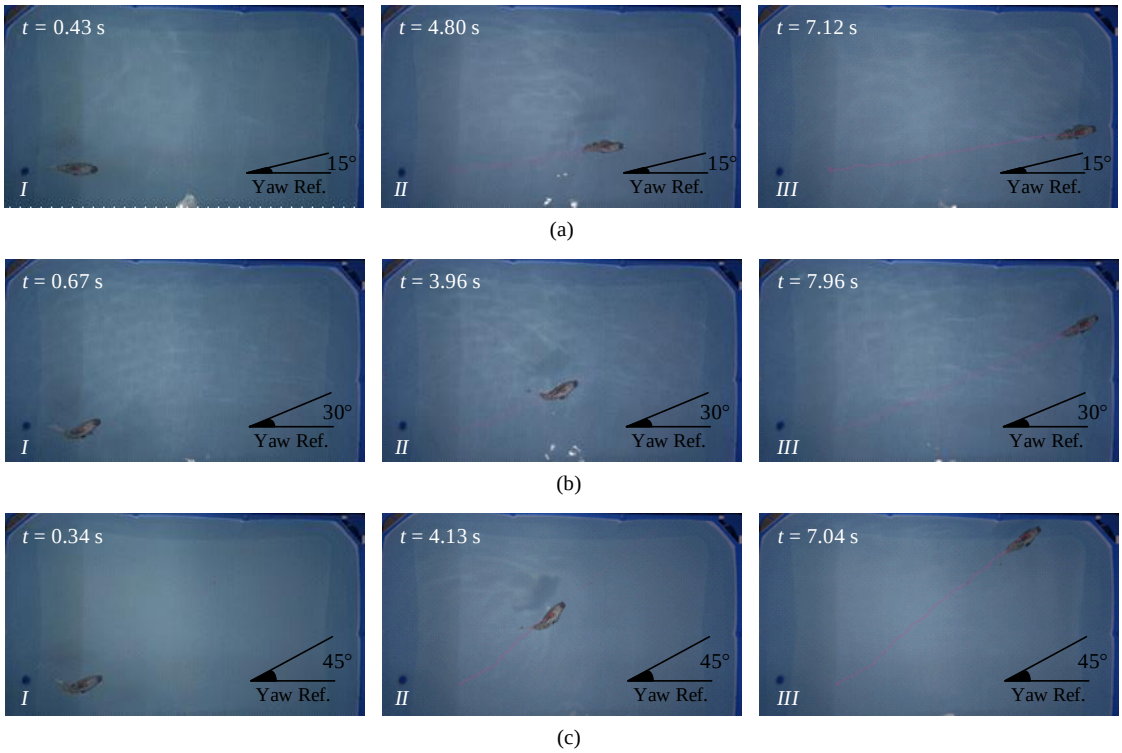

Figure 12. Experimental images of yaw control for Yaw Ref. = [15, 30, 45]°

The time-varying changes of the prototype positions with respect to these reference input variables are also presented in Figure 13 obtained by using Kinovea 0.8.26 program.

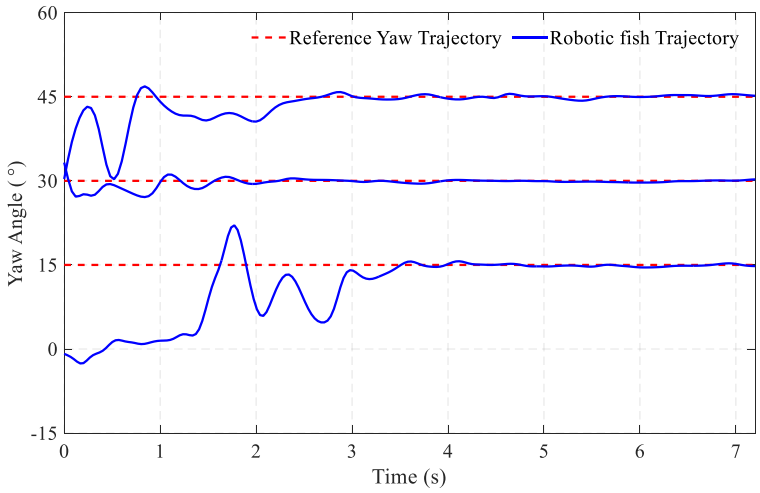

Figure 13. Experimental results of yaw control for various trajectories

As shown in Figure 13, the yaw angles of the robotic fish reach the desired reference input values and remain at the reference input values with small oscillations. When these results are examined, it is seen that the yaw control performance of the fuzzy controller is quite well.

The up/down motions of the robotic fish provide the third dimension capabilities. Experiments of the third dimension motion control are carried out for two different situations namely the pitch angle and the depth level control. For the control of the pitch angle, it is aimed to perform the descending motion while keeping the robot reference point at the desired reference pitch angles. In the depth level control experiments, it is aimed to keep the pitch angle at 0° in order to preserve the depth level of the robotic fish. The pitch angle values are received from the IMU sensor and evaluated according to the reference pitch angle, and the position of the sliding mass in the CoG control mechanism is changed by means of a proportional controller. As the position of the sliding mass changes, the CoG of the robot changes and thus the robotic fish realizes up/down motions. The linear motion of the sliding mass takes place on an endless screw shaft with a pitch of 5mm. This continuous rotation servo motor, which provides this shaft rotation, has 25.21 rpm rotation speed. Thus, the sliding mass moves linearly with velocity of 2.10 mm/s. The movement distance of the mass is approximately 28 mm.

Experiments on control of pitch angle to gain three-dimensional motion of the robot fish are performed for two different reference angles (-30° and -45°) considering the current conditions. For the analysis of these experiments, video images are recorded by means of two underwater action cameras. The obtained images are transferred to the Kinovea and a reference point is marked on the side surface of the robot fish prototype. The motion of the marked region is followed and the change in position of the robotic fish along the *x* and *y* axes is determined.

Images of experiments performed for the control of the pitch angle of the robot fish prototype are presented in Figure 14 for reference values of -30° and -45°.

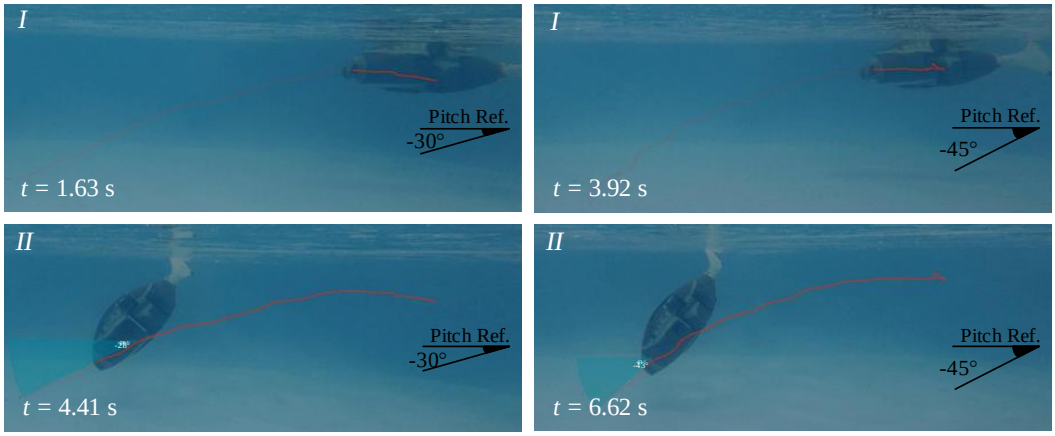

(a) (b)

Figure 14. Experimental images of pitch control for (a) Pitch Ref. = -30°; (b) Pitch Ref. = -45°

In Figure 14.a, the pitch angle control experiment with images for two different moments is performed over a 5 s period. It is observed that the prototype reaches to a steady state value at the end of 3 s when the curve of the path observed by the robotic fish is taken into consideration. Thus, using the Kinovea in the last 2 s of the view, the pitch angle value is obtained as -28°. The experiment shown in Figure 14.b is performed over a 7 s time period. It is observed that in the last 1 s of the experiment, the steady state angle reaches -43°.

Depth level control experiments are implemented to protect the level of the prototype at two different levels: near to base and near to surface. In these experiments, it is aimed to keep the pitch angle at zero to ensure the robot on the level. Images of the depth level control experiments near to base and surface and the time-dependent variation results of the obtained pitch angles are given in Figure 15.

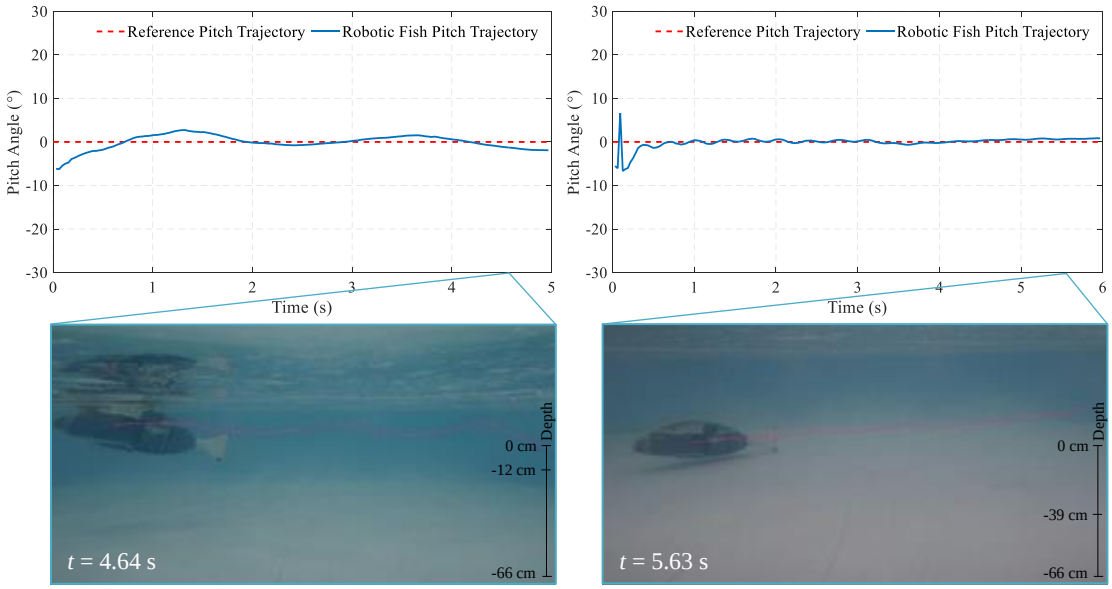

(a) (b)

Figure 15. Depth level control results: (a) image of near to surface experiment with pitch angle trajectory (depth level ≈ -12 cm); (b) image of near to base experiment with pitch angle trajectory (depth level ≈ -39 cm)

When the images of the control experiments of the depth level are examined, the average depth levels are calculated about -12 cm for near surface level and -39 cm for the near base level by using the Kinovea program. In addition, the pitch angles are about 0°.

It can be seen from the pitch angle and depth level control results that three-dimensional motion of the robotic fish is effectively achieved.

6. Conclusion

In this paper, hierarchal closed loop control structure is designed and three-dimensional locomotion of the robotic fish prototype is presented. Hierarchal control structure is developed by using a CPG, fuzzy logic and sensory feedback mechanism. The CPG model is inspired by the biological features of Lamprey spinal cord to generate rhythmic, robust and stable locomotion for effective swimming patterns. Fuzzy controller serves as a brain model of the robotic fish to decide necessary motion combinations according to sensory information. Sensory feedback mechanism is occurred from biological Lamprey sensory neurons to bring reflex of the prototype. The combination of these hierarchical control structure components behaves as a CNS. The CoG control mechanism is also developed for three-dimensional motion abilities of the robotic fish. Experimental results contain three specific swimming modes such as yaw, pitch and keep level and these experiments are performed with different scenarios. Yaw control is realized with three references. Pitch control is shown for two desired up/down motions and finally keep level is

achieved for near to base and near to surface. All results show that the proposed control structure achieves the effective and robust responses with real fish motions.

In the future work, three-dimensional trajectory tracking will be performed and swimming performance of the prototype will be examined with different intelligent control techniques.

Acknowledgement

This research was supported by the 114E652 TUBITAK 1001 project. We thank because of the financial support and guiding reports.

References

Ay M, Korkmaz D, Ozmen Koca G, Bal C, Akpolat Z, Bingol M. 2018. Mechatronic design and manufacturing of the intelligent robotic fish for bio-inspired swimming modes. Electronics, 7(7), 118.

Ay M, Ozmen Koca G, Korkmaz D, Bingol MC, Akpolat ZH. 2017. Prototype design and waterproof production of intelligent robotic fish (i-rof). 8th International Advanced Technologies Symposium. October 19-22, 2017. Elazig, Turkey:3960-3968.

Bing Z, Cheng L, Chen G, Röhrbein F, Huang K, Knoll A. 2017. Towards autonomous locomotion: cpg-based control of smooth 3d slithering gait transition of a snake-like robot. Bioinspiration and Biomimetics. 12(3):035001.

Crespi A, Lachat D. Pasquier A. 2008. Controlling swimming and crawling in a fish robot using a central pattern generator. Auton Robot. 25:3-13.

Ding R, Yu J, Yang Q, Tan M. 2013. Dynamic modelling of a cpg-controlled amphibious biomimetic swimming robot: Int J Adv Robot Syst. 10(4):1-11.

Hu Y, Liang J, Wang T. 2015. Mechatronic design and locomotion control of a robotic thunniform swimmer for fast cruising. Bioinspir Biomim. 10:026006.

Ijspeert AJ, Crespi A, Cabelguen JM. 2005. Simulation and robotics studies of salamander locomotion. Neuroinformatics. 3(3):171–195.

Ijspeert AJ. 2008. Central pattern generators for locomotion control in animals and robots: a review. Neural Networks. 21(4):642–653.

Korkmaz D, Ozmen Koca G, Bal C. 2018. Various applications of central pattern generators for locomotion control in robots: a review. Science and Eng. J of Firat Univ. 30(2):277-294.

Lachat D, Crespi A, Ijspeert AJ. 2006. BoxyBot: a swimming and crawling fish robot controlled by a central pattern generator. IEEE/RAS-EMBS Int Conf Bio Robot and Biomech.; February 20-22, 2006. Pisa, Italy:643-648.

Li G, Zhang H, Zhang J, Bye RT. 2014a. Development of adaptive locomotion of a caterpillar-like robot based on a sensory feedback cpg model. Adv Robot. 28(6):389–401.

Li G, Zhang H, Zhang J, Hildre HP. 2014b. An approach for adaptive limbless locomotion using a cpg-based reflex mechanism. J Bionic Eng. 11(3):389–399.

Li G. 2013. Hierarchical control of limbless locomotion using a bio-inspired cpg model. PhD Thesis: University of Hamburg.

Niu X, Xu J, Ren Q, Wang Q. 2014. Locomotion learning for an anguilliform robotic fish using central pattern generator approach. IEEE Transactions on Industrial Electronics. 61(9):4780-4787.

Ozmen Koca G, Bal C, Korkmaz D, Bingol M, A, M, Akpolat Z, Yetkin S. 2018. Three-dimensional modeling of a robotic fish based on real carp locomotion. Applied Sciences, 8(2), 180.

Ozmen Koca G, Bingol MC, Bal C, Akpolat ZH, Ay M, Korkmaz D. 2017. Design and control of diving mechanism for the biomimetic robotic fish. International Conference Mechatronics. Springer, Cham. September 13-15, 2017. Brno, Czech Republic:662-670.

Wang L, Wang S, Cao Z, Tan M, Zhou C, Sang H, Shen Z. 2005. Motion control of a robot fish based on cpg. Proc IEEE Int Conf Ind Technol. December 14-17, 2005. Hong Kong, China:1263–1268.

Wang T, Hu Y, Liang J. 2013. Learning to swim: A dynamical systems approach to mimicking fish swimming with cpg. Robotica. 31(3):361–369.

Wang W, Gu D, Xie G. 2017. Autonomous optimization of swimming gait in a fish robot with multiple onboard sensors. IEEE Transactions on Systems, Man, and Cybernetics: Systems. 49(5):1–13.

Wang W, Guo J, Wang Z, Xie G. 2013. Neural controller for swimming modes and gait transition on an ostraciiform fish robot. IEEE/ASME Int Conf Adv Intell Mechatronics. July 9-12, 2013. Wollongong, NSW, Australia:1564–1569.

Wang W, Xie G. 2014. CPG-based locomotion controller design for a boxfish-like robot. Int J Adv Robot Syst. 11:87.

Wu Q Di, Liu CJ, Zhang JQ, Chen QJ. 2009. Survey of locomotion control of legged robots inspired by biological concept. Sci China, Ser F Inf Sci. 52(10):1715–1729.

Wu Z, Yu J, Tan M, Zhang J. 2014. Kinematic comparison of forward and backward swimming and maneuvering in a self-propelled sub-carangiform robotic fish. J Bionic Eng. 11(2):199–212.

Wu Z, Yu J, Tan M. 2012. CPG parameter search for a biomimetic robotic fish based on particle swarm optimization. 2012 IEEE Int Conf Robot Biomimetics. December 11-14, 2012. Guangzhou, China:563–568.

Yu J, Tan M, Chen J, Zhang J. 2014. A survey on cpg-inspired control models and system implementation. IEEE Trans Neural Networks Learn Syst. 25(3):441–456.

Yu J, Wu Z, Wang M, Tan M. 2016. Cpg network optimization for a biomimetic robotic fish via pso. IEEE Transactions on Neural Networks and Learning Systems. 27(9):1962-1968.

Zhang D, Hu D, Shen Li, Xie H. 2006. A bionic neural network for fish-robot locomotion. J Bionic Eng. 3:187-194.

Zhang S, Qian Y, Liao P, Qin F, Yang J. 2016. Design and control of an agile robotic fish with integrative biomimetic mechanisms. IEEE/ASME Transactions on Mechatronics. 21(4):1846-1857.